Supporting Information

The synergy between atomically dispersed Pd and cerium oxide for enhanced catalytic properties

Xue Wang,*‡[ab] Jiayu Chen,‡[a] Jianxin Zeng,[a] Qiuxiang Wang,[a] Zejun Li,[c] Ruixuan Qin,[a] Changzheng Wu,[c] Zhaoxiong Xie*[a] and Lansun Zheng[a]

[a]State Key Laboratory of Physical Chemistry of Solid Surfaces, Collaborative Innovation Center of Chemistry for Energy Materials, and Department of Chemistry, College of Chemistry and Chemical Engineering, Xiamen University, Xiamen 361005, P. R. China

[b]State Key Laboratory for Oxo Synthesis and Selective Oxidation, Suzhou Research Institute, Lanzhou Institute of Chemical Physics, Chinese Academy of Sciences, Lanzhou 730000, P. R. China

[c]Hefei National Laboratory for Physical Sciences at the Microscale, Collaborative Innovation Center of Chemistry for Energy Materials, Hefei Science Center (CAS), and CAS Key Laboratory of Mechanical Behavior and Design of Materials, University of Science and Technology of China, Hefei 230026, P. R. China

‡ These authors contributed equally to this work.

*Correspondence to: zxxie@xmu.edu.cn; xuewang@licp.cas.cn

Experimental section:

Chemicals and materials.

Cerium(III) nitrate hexahydrate ($Ce(NO_3)_3 \cdot 6H_2O$), 1.00 M tetramethylammonium hydroxide (TMAH) aqueous solution, oleic acid, polyvinyl pyrrolidone (PVP, K-30), palladium(II) chloride ($PdCl_2$), L-ascorbic acid (AA), and benzyl alcohol (> 99%) were purchased from commercial suppliers (Alfa Aesar and Sinopharm Chemical Regent Co., Ltd.) and used as received without further purification. Chlorine acid palladium solution (H_2PdCl_4, 10 mM) was prepared by dissolving $PdCl_2$ (0.1773 g) in hydrochloric acid (HCl, 0.2 M, 10 mL) solution and then diluting it to 100 mL with deionized water.

Synthesis of CeO_2 truncated octahedra and cubes.

CeO_2 truncated octahedra and cubes were prepared based on the method reported in our previous study.[1] For the synthesis of CeO_2 truncated octahedra, 0.127 g of $Ce(NO_3)_3 \cdot 6H_2O$, 0.2 mL of 1.00 M TMAH aqueous solution, and 0.315 g of PVP were successively added to the mixture containing 3.0 ml of ethanol and 2.8 ml of distilled water under intense ultrasonic treatment. The resulting solution was then transferred to a 25 mL of Teflon-lined stainless steel autoclave and kept at 200 °C for 18 h. Finally, the products were collected by centrifugation at 10,000 rpm, and washed several times with ethanol.

For CeO_2 cubes, 0.127 g of $Ce(NO_3)_3 \cdot 6H_2O$, 1.10 mL of oleic acid, and 1.2 mL of 1.00 M TMAH aqueous solution were successively added to the mixture containing 2.7 ml of ethanol and 2.0 ml of distilled water under intense ultrasonic treatment. The resulting solution was transferred to a 25 mL of Teflon-lined stainless steel autoclave and kept at 200 °C for 18 h. The products were then collected by centrifugation at 10,000 rpm, and washed several times with cyclohexane and ethanol.

All the CeO_2 catalysts were dried at 50 °C and subsequently annealed at 400 °C for 1 h for use in the next step.

Synthesis of CeO_2 loaded with Pd by photochemical route.

0.14 g of CeO_2 was dispersed in 56.3 mL of deionized water, and then 1.316 mL of H_2PdCl_4 (10 mM) aqueous solution was added into the solution. The mixture magnetically stirred for 30 min in the dark. Then the solution was exposed to light irradiation for 30 min (I=10 mA).

A 300 W Xe lamp (PLS-SXE-300UV, Beijing Trusttech Co. Ltd) with a wavelength of 220–770 nm was employed as the light source. After reaction was finished, precipitate was collected by centrifugation at 6,000 rpm, and washed several times with deionized water. The sample was then dried under vacuum at ambient temperature.

Synthesis of CeO_2+H_2PdCl_4 catalysts.

0.14 g of CeO_2 was dispersed in 56.3 mL of deionized water, and then 1.316 mL of H_2PdCl_4 (10 mM) aqueous solution was added into the solution. The mixture magnetically stirred for 1 h in the dark. The precipitate was collected by centrifugation at 6,000 rpm, and washed several times with deionized water. The sample was then dried under vacuum at ambient temperature.

Synthesis of CeO_2 loaded with Pd by chemical reduction.

0.14 g of CeO_2 was dispersed in 56.3 mL of deionized water, and 1.316 mL of H_2PdCl_4 (10 mM) aqueous solution was added. After the mixture was magnetically stirred for 30 min in the dark, 0.443 mL of AA (0.1 M) aqueous solution was added in the solution by dropwise. The final solution magnetically stirred for 6 h at 30 °C. After reaction was finished, precipitate was collected by centrifugation at 6,000 rpm, and washed several times with deionized water. The sample was then dried under vacuum at ambient temperature.

Characterization.

The morphology and crystal structure of the as-prepared products were observed by HRTEM, (JEM 2100) with an acceleration voltage of 200 kV. HAADF-STEM and EDX analyses were carried out on a FEI TECNAI F20 microscope operated at 200 kV. All TEM samples were prepared by depositing a drop of diluted suspension in distilled water on a copper grid coated with carbon film. The surface structure for desired nanocatalysts was analyzed by XPS, which was carried out in a UHV system using a monochromatised Al Kα radiation (hν=1486.6 eV). The binding energies were calibrated with respect to the signal for adventitious carbon (binding energy of 284.6 eV). The precise contents of Pd element in samples were determined by ICP-AES (Baird PS-4).

The X-ray absorption spectra (XAS) at the Pd K-edge measurements were performed in fluorescence mode at the BL14W1 beamline of the Shanghai Synchrotron Radiation Facility. The energy of the storage ring was 3.5 GeV in SSRF. Si(311) double-crystal monochromator

was calibrated by Pd foil and the XAS data of Pd foil and PdO standard were collected for the reference spectrum. All the spectra were recorded in ambient conditions.

The XAS data processing was conducted in Demeter (version 0.9.25). The obtained XAS original data was processed for the background, pre-edge line, post-edge line correction and normalized in Athena. The EXAFS fitting was conducted in Artemis. The model Pd (EntryWithCollCode41517.cif) and PdO (EntryWithCollCode185482.cif) were used as the FEFF input file. The Pd-O-Ce model was manually wrote into the FEFF input file, according to the model shown in Fig. 4c. The $\chi(k)$ data was then transformed into R-space using Fourier transformation, and a k range of 3-13 $Å^{-1}$ and k-weighting of 2 were used for all the samples. The data of Pd foil was firstly fitted with the Pd-Pd coordination number set as 12, and then the amplitude reduction factor (S_0^2) was determined to be 0.83 (single scattering fitting, R range 1.0-2.5 Å uncorrected), which was used for all the other data fitting process. The data of PdO was fitted with Pd-O for the first shell and Pd-Pd for the second shell (R range 1.0-3.5 Å uncorrected). Multi-scattering fitting had been tried for four types of Pd/CeO_2 catalysts, but no good fitting result was obtained. Then two-shell single-scattering fitting was used for these four types of Pd/CeO_2 catalysts. For Pd/CeO_2-TOC and Pd/CeO_2-CC, the first and second shells fitted with Pd-O and Pd-Pd scattering, respectively, with R range of 1.0-3.0 Å. For Pd/CeO_2-TOP and Pd/CeO_2-CP, the first shell fitted with Pd-O scattering, and the fit for the second shell was tried by using Pd-Pd and Pd-Ce scattering, respectively, with R range of 1.0-3.5 Å. The four parameters (coordination number (CN), bonding distance (R), Debye–Waller factor (σ^2), and shift in adsorption edge energy (E_0)) for each shell were fitted without any fixed, constrained, or correlated.

Fourier transform infrared spectra were recorded on a Thermo Nicolet 6700 equipped with an *in situ* reaction chamber. Samples were prepared by mixing catalysts and KBr according to the weight ratio of 1:10. Before CO adsorption, the cell was evacuated at room temperature for 30 min and then a background spectrum was taken. CO (99.999%) controlled by a mass flow meter was fed at a flow rate of 80 mL min^{-1} for 10 min. The spectra were measured by accumulating 64 scans at a spectra resolution of 8 cm^{-1} and were recorded at room temperature.

CO Oxidation Reaction.

The catalytic activity of catalysts towards CO oxidation was performed in a continuous flow reactor. The reaction gases, 5% CO in nitrogen (99.999%) (10 mL min^{-1}) and air (99.999%) (40 mL min^{-1}), were fed to 100 mg of catalysts set in a fixed-bed flow reactor made of glass with an inner diameter of 2.4 mm. Steady-state catalytic activity was measured at each temperature, with the reaction temperature rising from room temperature to 130 °C in step of 10 °C. The effluent gas was analysed on-line by an on-stream gas chromatograph (Ramiin GC 2060) equipped with a TDX-01 column.

Benzyl Alcohol Reaction.

80 mg of catalyst was dispersed in 3 mL of benzyl alcohol (29.0 mmol) in a three-necked flask connected to O_2. Before the reaction, O_2 was pumped into the solution at a rate of 20 mL min^{-1} for half an hour to get rid of the air. The reaction was then operated at 80 °C for different reaction times with stirring under reflux. The O_2 was kept purging in the solution during the reaction process. After the reaction, the liquid mixture was obtained through centrifugation, followed by sieve filtration to remove catalysts. Product was separated into two parts for analyses and dodecane was used as internal standard substance. For one part, 75.5 μL dodecane was added into 924.5 μL product. For the other, 200 μL product was added into the mixture of 2347.4 μL CH_2Cl_2 and 227.6 μL dodecane. The product was analyzed on-line by on-stream gas chromatographs (Shimadzu GC-2014C and Shimadzu GC-2010-MS) equipped with capillary columns (KB-5MS, 30m × 0.32 mm for GC-2014C; RTS-5MS, 30m × 0.32 mm for GC-2010-MS).

References:

1 X. Wang, Z. Jiang, B. Zheng, Z. Xie and L. Zheng, *CrystEngComm*, 2012, **14**, 7579–7582.

2 E. A. Stern, M. Newville, B. Ravel, Y. Yacoby and D. Haskel, *Physica B*, 1995, **208-209**, 117−120.

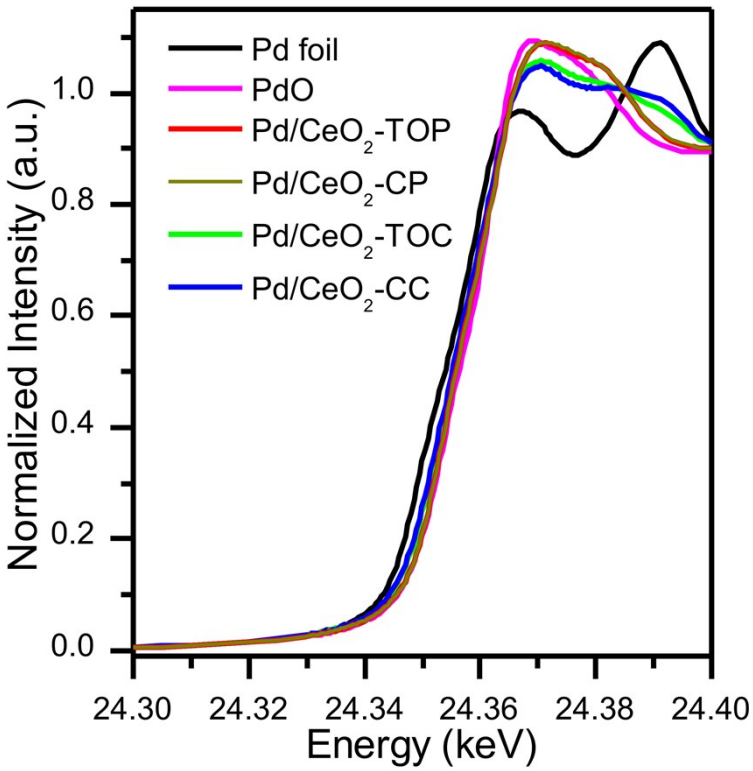

Figure S1. The normalized XANES spectra at the Pd K-edge of different Pd/CeO_2 samples as well as of reference materials Pd foil and PdO. In comparison with Pd foil, the main edges of four types of Pd/CeO_2 shifted to higher energy, indicating that the average oxidation state of Pd in Pd/CeO_2 samples was higher than that of Pd^0. The main edges of Pd/CeO_2-TOP and Pd/CeO_2-CP almost overlapped with that of PdO, suggesting that the average oxidation state of Pd in Pd/CeO_2-TOP and Pd/CeO_2-CP were close to +2. Relative to Pd/CeO_2-TOP and Pd/CeO_2-CP, lower energy for adsorption edges of Pd/CeO_2-TOC and Pd/CeO_2-CC presented lower oxidation state of Pd.

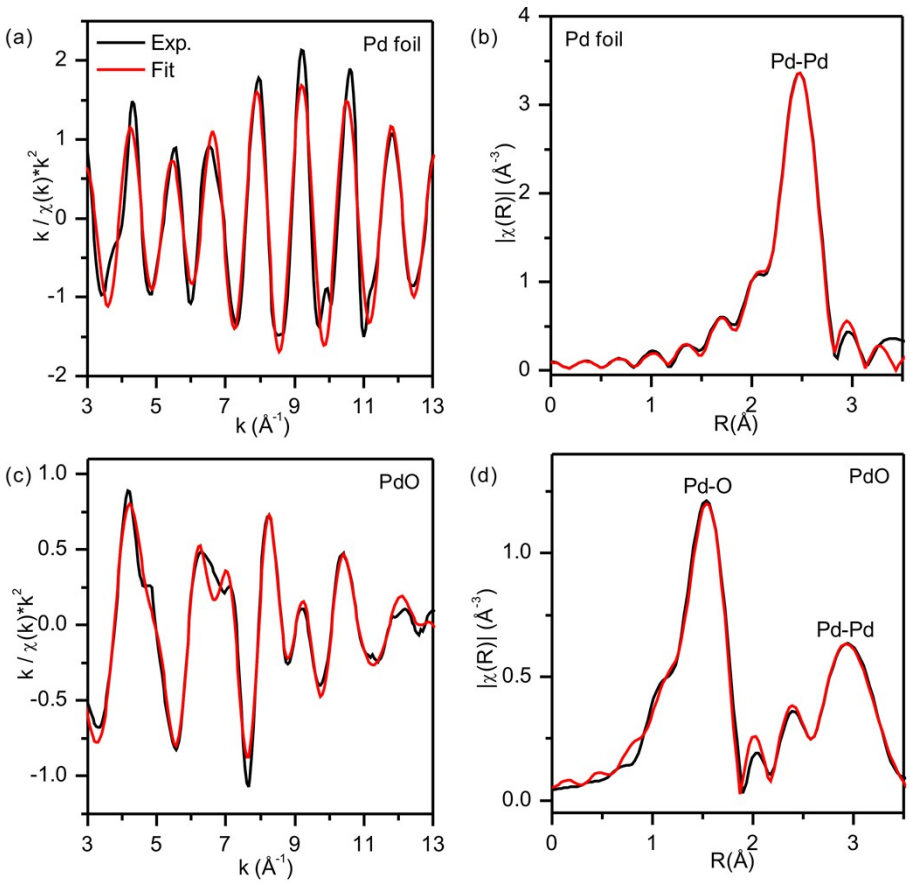

Figure S2. (a) EXAFS k-space and (b) R-space fitting for reference material Pd foil at the Pd K-edge. (c) EXAFS k-space and (d) R-space fitting for PdO at the Pd K-edge. The color scheme in (a) applies to all other panels. The quantified fitting results are shown in Table S3.

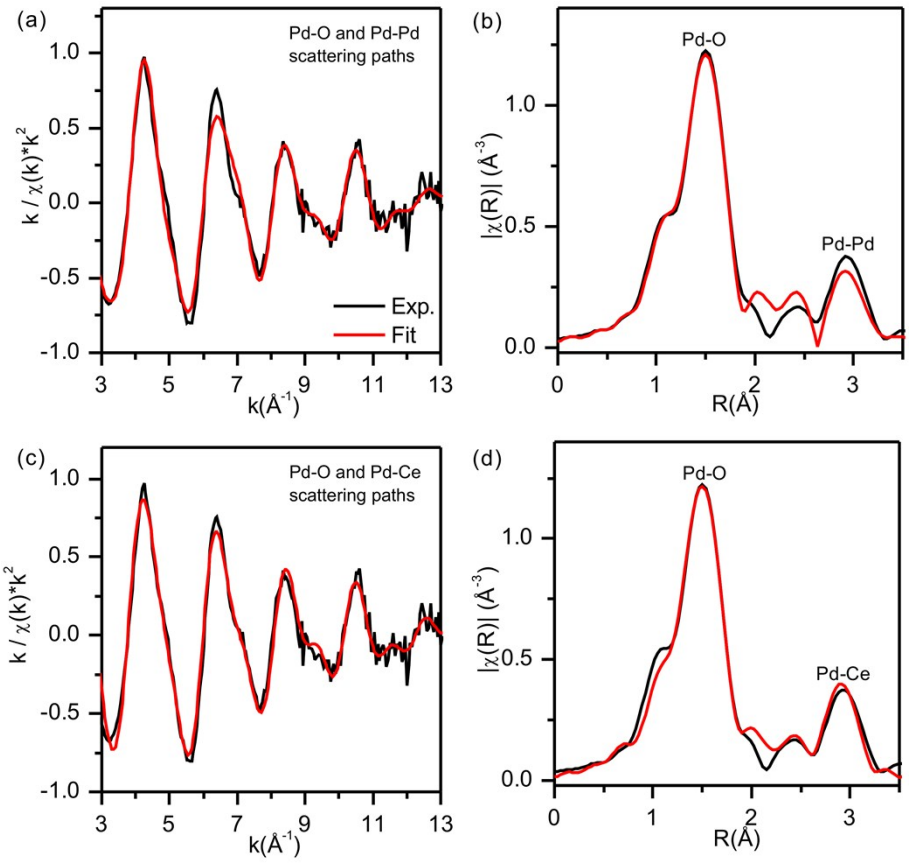

Figure S3. (a) EXAFS k-space and (b) R-space fitting with Pd-O and Pd-Pd scattering paths for Pd/CeO_2-TOP. (c) EXAFS k-space and (d) R-space fitting with Pd-O and Pd-Ce scattering paths for Pd/CeO_2-TOP. The color scheme in (a) applies to all other panels. The quantified fitting results are shown in Table S4. The fitting results showed that Pd-Ce scattering path fitting with less R-factor and reduced chi-square was better than Pd-Pd scattering path fitting for the peak at ~ 3 Å (uncorrected) in R-space, confirming the single-atom-dispersed Pd in Pd/CeO_2-TOP.

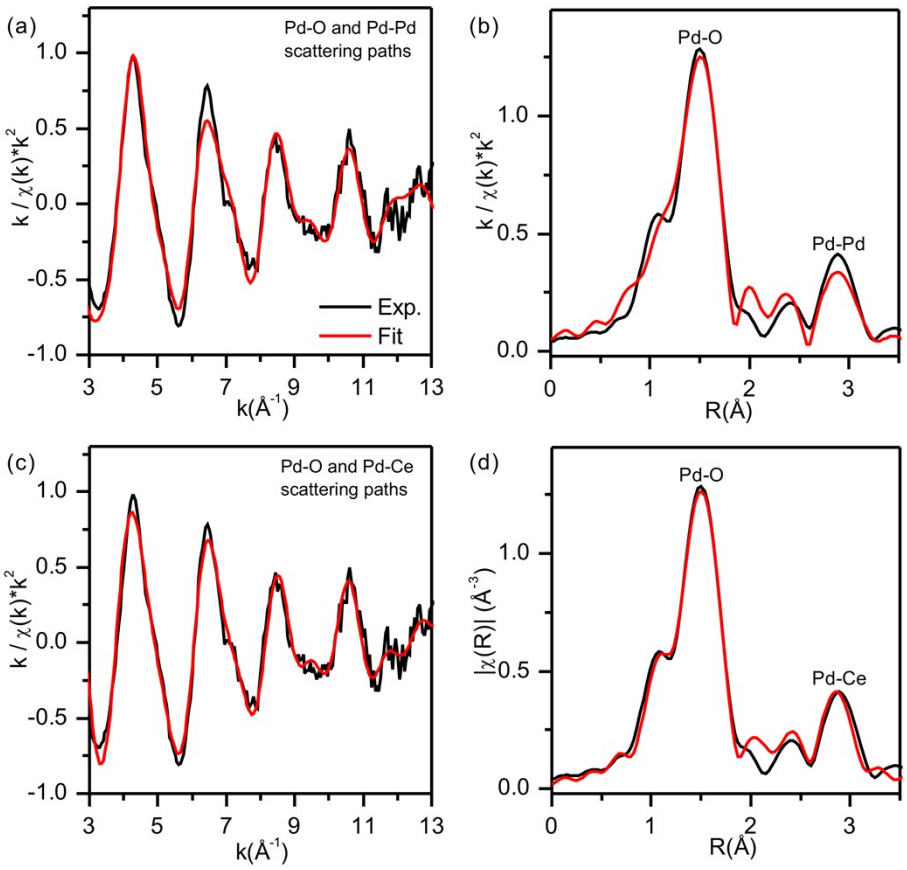

Figure S4. (a) EXAFS k-space and (b) R-space fitting with Pd-O and Pd-Pd scattering paths for Pd/CeO_2-CP. (c) EXAFS k-space and (d) R-space fitting with Pd-O and Pd-Ce scattering paths for Pd/CeO_2-CP. The color scheme in (a) applies to all other panels. The quantified fitting results are shown in Table S4. The fitting results also showed that Pd-Ce scattering path fitting with less R-factor and reduced chi-square was better than Pd-Pd scattering path fitting for the peak at ~ 3 Å (uncorrected) in R-space, confirming the single-atom-dispersed Pd in Pd/CeO_2-CP.

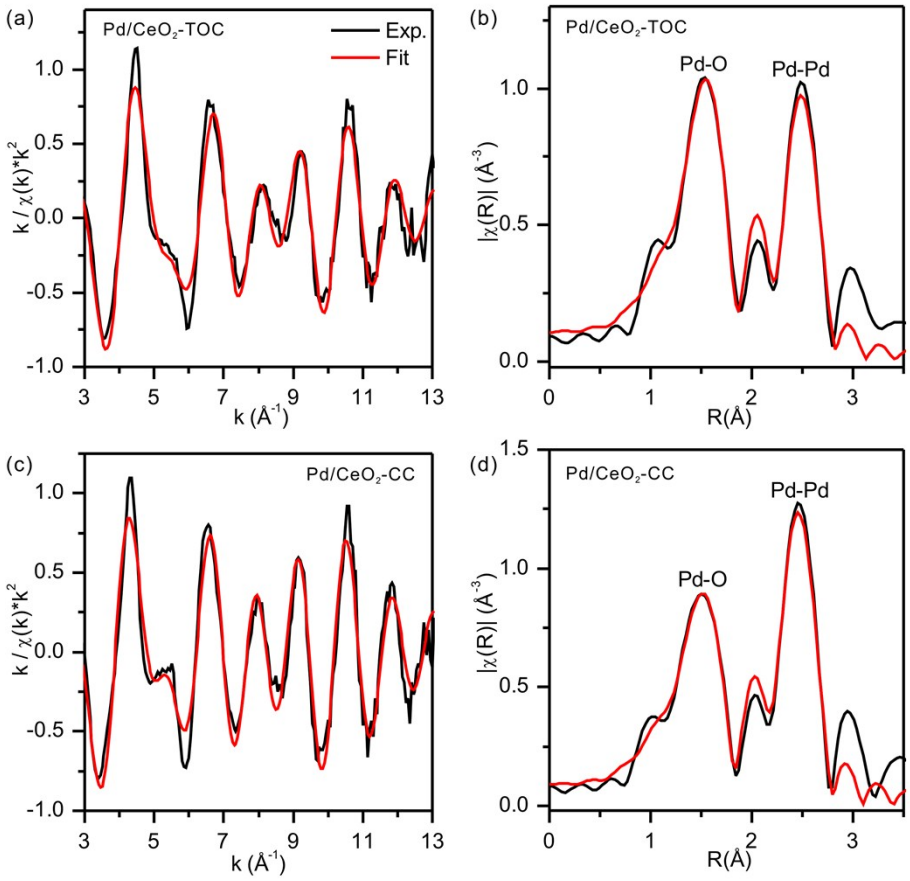

Figure S5. (a) EXAFS k-space and (b) R-space fitting for Pd/CeO_2-TOC at the Pd K-edge. (c) EXAFS k-space and (d) R-space fitting for Pd/CeO_2-CC at the Pd K-edge. The color scheme in (a) applies to all other panels. The quantified fitting results are shown in Table S3. For R-space fitting, the peaks at ~ 1.5 Å (uncorrected) and ~ 2.5 Å (uncorrected) were attributed to Pd-O and Pd-Pd scattering, respectively.

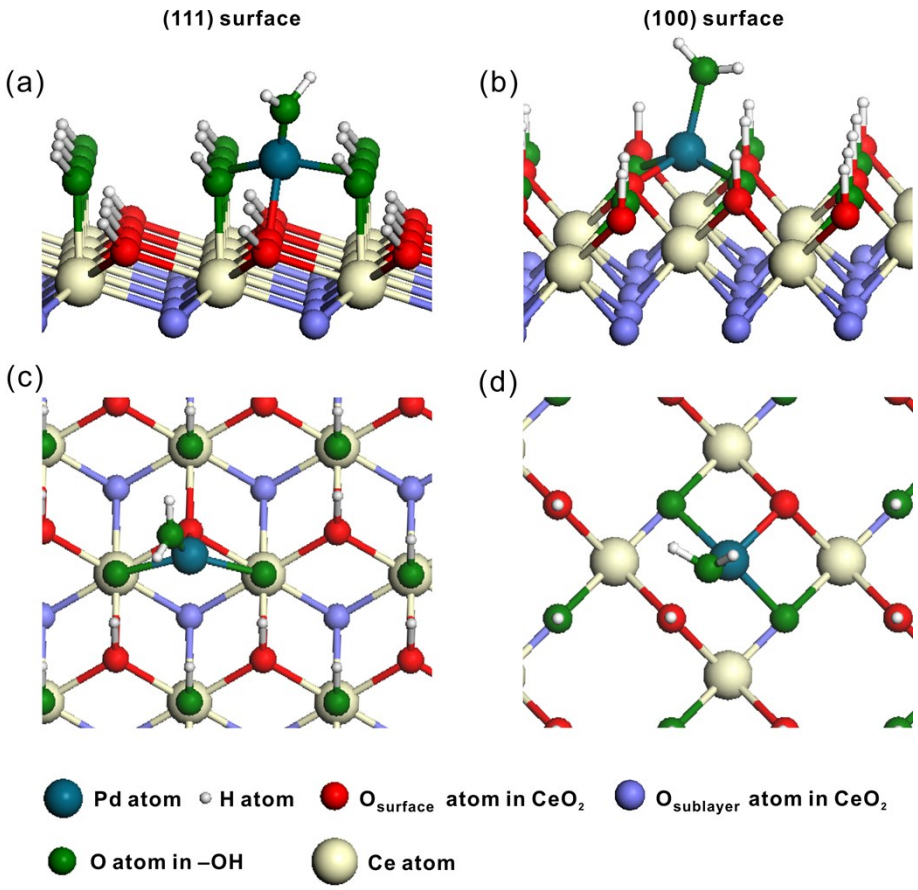

Figure S6. Side views of possible schematic structure models for (a) $Pd_1/CeO_2(111)$ and (b) $Pd_1/CeO_2(100)$. Top views of possible schematic structure models for (c) $Pd_1/CeO_2(111)$ and (d) $Pd_1/CeO_2(100)$.

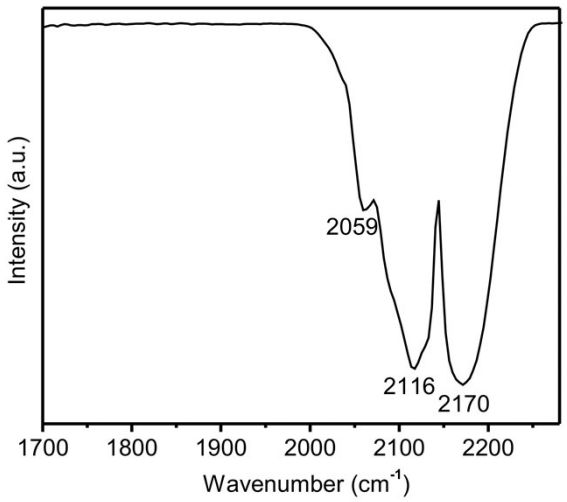

Figure S7. FTIR spectra of CO adsorption on Pd/CeO_2-TOP. The bands at 2059, 2116, and 2170 cm^{-1} can be ascribed to CO linearly adsorbed on Pd^0, Pd^+, and Pd^{2+}, respectively.

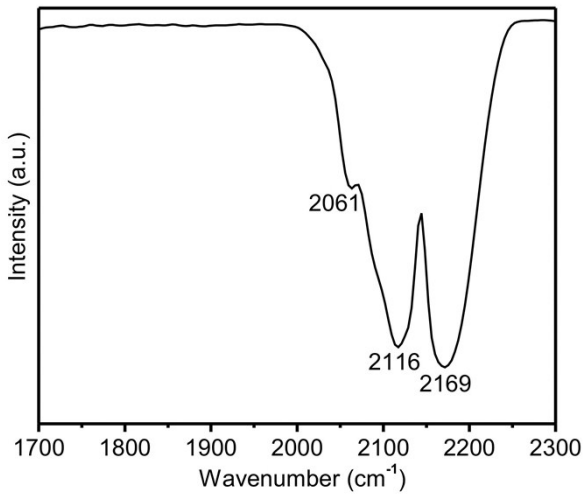

Figure S8. FTIR spectra of CO adsorption on Pd/CeO_2-CP. The bands at 2061, 2116, and 2169 cm^{-1} can be ascribed to CO linearly adsorbed on Pd^0, Pd^+, and Pd^{2+}, respectively.

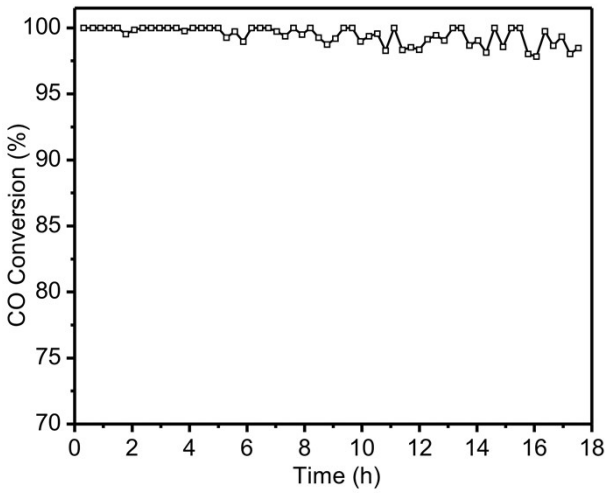

Figure S9. Catalytic performance of Pd/CeO_2-TOP at 90 °C in CO oxidation.

Table S1. Summary of the weight percentages of Pd in different Pd/CeO_2 catalysts.

Samples	Pd/CeO_2-TOP	Pd/CeO_2-CP	Pd/CeO_2-TOC	Pd/CeO_2-CC
wt% of Pd from ICP-AES	0.88	0.89	0.84	0.84

Table S2. Results of curve fitting of Pd 3d XPS spectra for different Pd/CeO_2 catalysts.

Samples		Oxidized Pd single atom or clusters	Pd^{2+} located in $Pd_xCeO_{2-\delta}$
Pd/CeO_2-TOP	binding energy / eV	336.0/341.1	337.4/342.6
	relative percentage (%)	15.4%	84.6%
Pd/CeO_2-CP	binding energy / eV	336.1/341.2	337.5/342.7
	relative percentage (%)	30.3 %	69.7%
Pd/CeO_2-TOC	binding energy / eV	335.8/341.0	337.5/342.6
	relative percentage (%)	60.8 %	39.2%
Pd/CeO_2-CC	binding energy / eV	335.8/341.0	337.6/342.8
	relative percentage (%)	59.8%	40.2%

Table S3. EXAFS parameters of bulk Pd foil, PdO, Pd/CeO_2-TOC, and Pd/CeO_2-CC.

Samples	Shell	CN	R (Å)	$\sigma^2 \times 10^3$ ($Å^2$)	ΔE_0 (eV)	R-factor
Pd foil	Pd-Pd	12*	2.74±0.00	5.4±0.2	-5.2±0.2	0.011
PdO	Pd-O	3.6±0.3	2.02±0.01	1.7±0.8	-0.9±1.4	0.007
	Pd-Pd	2.8±1.6	3.03±0.03	5.5±2.9	-0.9±4.8	
	Pd-Pd	4.5±2.4	3.44±0.04	7.3±3.3	-2.3±5.3	
Pd/CeO_2-TOC	Pd-O	2.8±0.3	2.00±0.01	2.0±1.2	4.5±1.7	0.007
	Pd-Pd	2.8±0.5	2.74±0.01	4.7±1.1	-1.0±1.8	
Pd/CeO_2-CC	Pd-O	2.5±0.3	2.00±0.01	2.0±1.2	0.0±2.0	0.005
	Pd-Pd	3.9±0.5	2.74±0.00	5.0±1.2	-6.6±1.2	

R-factor is given to show the goodness of fit parameter. Generally, the fit is considered to be good if R-factor is no more than 0.02, and the fit is better with less R-factor.[2] As all the R-factors in Table S3 are less than 0.02, the fits for Pd, PdO, Pd/CeO_2-TOC, and Pd/CeO_2-CC are good.

*Based on the known structure of Pd, this value was fixed during EXAFS fitting.

In above table, the low coordination number of Pd-Pd in Pd/CeO_2-TOC and Pd/CeO_2-CC may result from the average effect of Pd nanoparticles and Pd clusters on CeO_2 supports.

Table S4. EXAFS parameters of Pd/CeO_2-TOP and Pd/CeO_2-CP by using two types of scattering path fitting.

Samples	Scattering path	Shell	CN	R (Å)	$\sigma^2 \times 10^3$ (Å^2)	ΔE_0 (eV)	R-factor	χ_v^2
Pd/CeO_2-TOP	Pd-O and Pd-Pd scattering paths	Pd-O	4.8±0.6	2.01±0.01	4.2±1.4	-2.9±1.8	0.023	32
		Pd-Pd	2.1±1.1	3.10±0.02	8.0±3.6	14.0±3.3		
	Pd-O and Pd-Ce scattering paths	Pd-O	5.5±0.6	2.00±0.01	5.1±1.1	-12.0±1.4	0.015	21
		Pd-Ce	3.1±1.2	3.32±0.02	7.1±2.6	-8.5±2.9		
Pd/CeO_2-CP	Pd-O and Pd-Pd scattering paths	Pd-O	4.7±0.6	2.00±0.01	3.8±1.3	-2.7±1.7	0.023	50
		Pd-Pd	2.1±1.0	3.06±0.02	7.5±3.3	13.7±3.2		
	Pd-O and Pd-Ce scattering paths	Pd-O	5.3±0.7	2.00±0.01	4.5±1.3	-11.8±1.7	0.020	44
		Pd-Ce	3.1±1.3	3.20±0.02	8.7±2.8	-9.1±3.4		

χ_v^2, reduced chi-square. χ_v^2 depends on the uncertainty in the data and the fit is better with lower χ_v^2.

The notable peaks at ~ 1.5 Å were from Pd-O scattering contribution. For the peak at ~ 3 Å (uncorrected) in R-space, both Pd-Pd and Pd-Ce scattering path fittings were tried and compared (Fig. S3 and S4†), and it showed that Pd-Ce scattering path fitting with less R-factor and χ_v^2 was better than Pd-Pd scattering path fitting, confirming the atomically dispersed Pd for Pd/CeO_2-TOP and Pd/CeO_2-CP.

Table S5. Calculated TOFs based on all Pd atoms for different Pd/CeO_2 catalysts at 90 °C.

Samples	Pd/CeO_2-TOP	Pd/CeO_2-CP	Pd/CeO_2-TOC	Pd/CeO_2-CC
TOF (h^{-1})	1619	1103	28	5

Table S6. Activity and selectivity of CeO_2-H_2PdCl_4 catalysts toward benzyl alcohol oxidation at 80 °C for 5 h.

Samples	Conversion (%)	Selectivity (%)			TOF[a] (h^{-1})
		Benzaldehyde	Toluene	Benzoic acid	
Truncated octahedral CeO_2 + H_2PdCl_4	19.7	96.8	3.2	−	202
Cubic CeO_2 + H_2PdCl_4	0.9	100	−	−	12

a TOF for benzaldehyde production, calculated based on all Pd atoms measured by ICP-AES after 5 h of reaction.